

Temperature of the plume layer beneath the Yellowstone hotspot

Derek L. Schutt*, Ken Dueker

University of Wyoming, Department of Geology and Geophysics, 1000 University Avenue, Laramie, Wyoming 82071, USA

ABSTRACT

Recent studies show that the Yellowstone hotspot is associated with a plume-like low-velocity pipe that ascends from the transition zone to the lithosphere-asthenosphere boundary, where the plume is sheared to the southwest by North American plate motion. Rayleigh wave tomography shows this plate-sheared plume layer has an extremely low S wave velocity of 3.8 ± 0.1 km/s at 80 km depth, ~0.15–0.3 km/s lower than the velocity observed beneath normal mid-ocean ridges. To constrain the temperature of the plume layer, a grid search with respect to grain size and temperature is performed to fit the observed Rayleigh wave phase velocities. This search finds that the excess temperature of the plume layer is >55–80 °C at 95% confidence for two different temperature-velocity and two different melt-velocity models, confirming that a thermal mantle plume exists.

Keywords: Yellowstone, plume, Snake River Plain, temperature, grain size, tomography.

INTRODUCTION

A recent deployment of seismometers in the Yellowstone area (Wyoming, USA) has provided an excellent new data set with which to examine the deep structure of the hotspot (Fig. 1). Studies utilizing these data have found a relatively low P wave and S wave velocity pipe that extends from 500 to 600 km depth to ~60 km depth, where it is sheared to the southwest by North American plate motion (Fee and Dueker, 2004; Waite et al., 2006; Yuan and Dueker, 2005). Based on fundamental mode Rayleigh wave measurements, the plate-sheared plume layer has been found to have an extremely low shear velocity of 3.8 ± 0.1 km/s (Schutt et al., 2008). This velocity is 0.15–0.3 km/s lower than imaged by Rayleigh waves beneath normal mid-ocean ridges (Nishimura and Forsyth, 1989; Weeraratne et al., 2007) and 0.3–0.4 km/s lower than a 1320 °C potential temperature adiabatic mantle (Cammarano et al., 2003; Schutt and Lesher, 2006). While these low upper mantle velocities along the Yellowstone hotspot track suggest a plume, modeling of the effects of different anelastic velocity models and melt porosity is required to quantitatively assess the temperature of the low-velocity sheared plume layer beneath the Yellowstone hotspot track, and thus the minimum temperature of the plume layer. Constraining the temperature of the plume layer beneath the hotspot track is of particular interest since the plume conduit is suggested to end in the transition zone and to not extend into the lower mantle (Montelli et al., 2004b; Waite et al., 2006; Yuan and Dueker, 2005). In addition, because mantle with an excess potential temperature must ultimately come from a thermal boundary layer, a finding of significant excess temperature would further argue against studies that suggest a non-plume origin for the Yellowstone hotspot track (Christiansen et al., 2002). For example, processes such as small-scale convection (King and Ritsema, 2000) or lithospheric extension would produce temperature variations, but would not produce temperatures in excess of the potential temperature of ambient mantle, since they cannot create excess temperature mantle.

Schutt et al. (2008) measured fundamental mode Rayleigh waves using the two plane wave technique of Forsyth and Li (2005). In that study, Rayleigh wave observations were inverted for phase velocity as a function of wave period in three tectonic regions: the Yellowstone hotspot track, which overlies the plate-sheared plume layer; the immediately adjacent Basin and Range; and the Wyoming craton, which is

unaffected by the Yellowstone plume (Fig. 1). Phase velocity was then inverted for shear wave velocity (V_S) as a function of depth for each region (Schutt et al., 2008).

In this study we forward model the effects of plume temperature on S wave velocity, convert this to phase velocity, and compare these predictions to observations. To accomplish this task, a four-layer S wave velocity model is constructed to represent the Yellowstone hotspot track crust, mantle lithosphere, plume layer, and subplume mantle (Fig. 2A). To reduce tradeoffs between the model parameters, the velocity of the crust, mantle lithosphere, and subplume mantle is fixed as discussed below. For

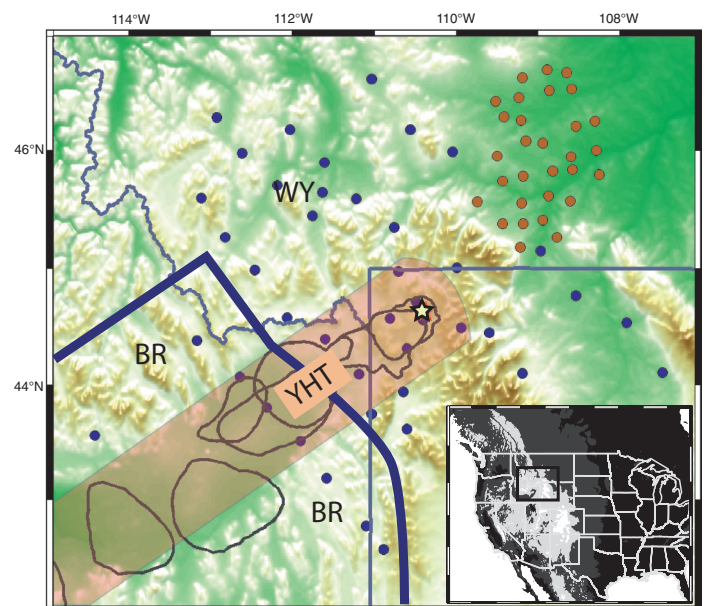
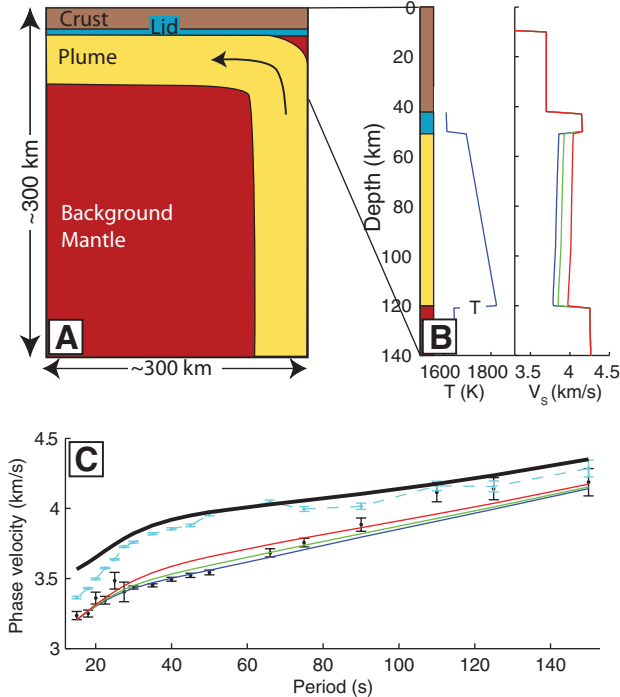


Figure 1. Elevation, seismic stations, and tectonic regions covered by Yellowstone array. Tectonic regions have been defined as follows: pink swath is Yellowstone hotspot track (YHT), which includes the eastern Snake River Plain and Yellowstone Park; dark blue line outlines Basin and Range (BR); rest of the area is assigned to Wyoming craton (WY). Blue and red circles denote the Billings and Yellowstone arrays, respectively. Black and white inset shows location of larger map in the context of western United States.

*Current address: Department of Geosciences, Warner College of Natural Resources, Colorado State University, Colorado 80523-1482, USA.



melt-velocity scaling relation of Kreutzmann et al. (2004). The following quantities are used: F-test (black lines), melt porosity at top of plume layer (red lines), and reduced chi-squared misfit (χ^2_v) for grain-size-sensitive anelastic model using grain-size-sensitive anelastic velocity scaling for grain sizes of 2 mm (blue), 3 mm (green), and 7 mm (red). C: Predicted phase velocities for the three example V_s models shown in B and observations with their one standard error bars. Cyan dashed line and black solid lines are for Wyoming craton and Preliminary Reference Earth Model (PREM) (Dziewonski and Anderson, 1981) velocity models. D: Reduced chi-squared error surface for grain-size-sensitive anelastic model using grain-size-sensitive anelastic velocity scaling for grain sizes of 2 mm (blue), 3 mm (green), and 7 mm (red). E: Same plot as D, except that the non-grain-size-sensitive anelastic model is used (Karato, 1993).

the plume layer, the temperature and grain size are varied in a grid search. Each temperature and grain size combination is converted to V_s , and the phase velocities are calculated. In addition, the velocity reduction associated with the equilibrium melt porosity is calculated based on the grain size and vertical Darcy Law flow (Turcotte and Schubert, 2002). The reduced chi-squared misfit (denoted as χ^2_v) is calculated permitting F-test-based confidence intervals to be evaluated (Figs. 2A–2C). Details of the model are presented in the Appendix (GSA Data Repository¹).

MODELING THE EFFECTS OF TEMPERATURE AND GRAIN SIZE

Different shear velocity scaling relations have been proposed for the effects of melt porosity, temperature, and grain size, and will affect our conclusions. In addition, the presence of water could also affect velocity, but the removal of significant amounts of melt is predicted to dehydrate the mantle (Schutt and Humphreys, 2004). Therefore, we discount the effects of water and have chosen to test the most commonly used scaling relations (Table 1). Melt porosity effects on velocity are calculated using two different models (Hammond and Humphreys, 2000; Kreutzmann et al., 2004). To translate temperature to velocity, both elastic and anelastic effects are assessed. The elastic velocity component is straightforward to calculate for a pyrolytic mantle composition (Schutt and Lesher, 2006). The anelastic velocity component is less certain, so three models of anelasticity are considered: a grain-size-sensitive (GSS) laboratory-based model (Faul and Jackson, 2005), a non-grain-size-sensitive (NGSS) theoretical model (Goes et al., 2000; Karato, 1993; Minster and Anderson, 1981), and an empirical relation calibrated to

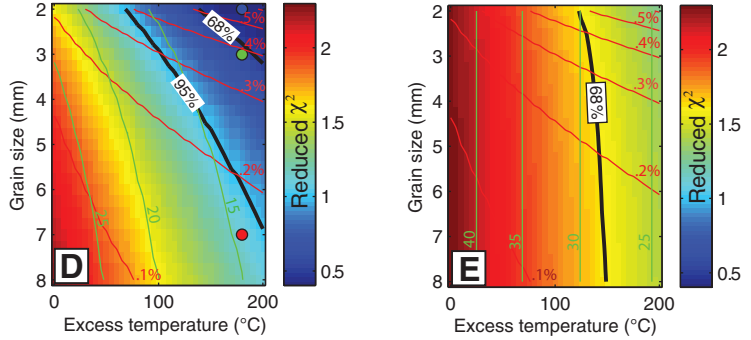


Figure 2. Yellowstone plume layer temperature, melt porosity, and shear wave attenuation. A: Cross section along Yellowstone hotspot track from surface wave tomography. B: Hotspot structure is approximated by four layers: crust, mantle lid, plate-sheared plume layer, and underlying mantle. Example thermal profile is shown for 180 °C excess temperature (T). Temperature decreases within plume layer are due to latent heat of melting. Colored lines in plume layer are example V_s profiles calculated for this temperature structure using grain-size-sensitive anelastic velocity scaling for grain sizes of 2 mm (blue), 3 mm (green), and 7 mm (red). C: Predicted phase velocities for the three example V_s models shown in B and observations with their one standard error bars. Cyan dashed line and black solid lines are for Wyoming craton and Preliminary Reference Earth Model (PREM) (Dziewonski and Anderson, 1981) velocity models. D: Reduced chi-squared error surface for grain-size-sensitive anelastic model using grain-size-sensitive anelastic velocity scaling for grain sizes of 2 mm (blue), 3 mm (green), and 7 mm (red). E: Same plot as D, except that the non-grain-size-sensitive anelastic model is used (Karato, 1993).

ocean-basin shear wave velocities, assumed thermal models, and xenolith constraints (Priestley and McKenzie, 2006).

Without independent constraints such as seismic attenuation, the velocity tradeoff between grain size and temperature variations cannot be uniquely resolved. For example, for the GSS anelastic model, a 100 °C increase in temperature is equivalent to a reduction in the grain size from 8 to 2 mm (Fig. 2D). Thus, we have been forced to choose a minimum plume layer grain size to constrain a minimum excess temperature estimate. If stress and crystal size are inversely correlated (e.g., Hall and Parmentier, 2003), and the cold lithosphere has higher stresses than the asthenosphere, then lithospheric grain sizes serve as a minimum bound for those in the asthenosphere. Xenoliths from the base of the lithosphere typically have a 0.5–2 mm grain size (Armienti and Tarquini, 2002; Wilshire et al., 1988), and 2 mm is adopted as a lower asthenospheric grain-size bound. There is no well constrained upper grain-size bound, although for grain sizes >8 mm, an excess plume layer temperature of >200 °C would be required. Such a large excess temperature

TABLE 1. TEMPERATURE CONSTRAINTS FOR DIFFERENT SCALING MODELS

	95% confidence	68% confidence	95% confidence χ^2_v	68% confidence χ^2_v
GSS				
$d\ln V_s/dF = 2.1^*$	70°	135°	1.0	0.5
$d\ln V_s/dF = 7.9^{\dagger}$	55°	160°	0.9	0.5
NGSS				
$d\ln V_s/dF = 2.1^*$	N/A	120°	2.3	1.6
$d\ln V_s/dF = 7.9^{\dagger}$	70°	170°	1.7	0.9

Note: A grain size of 2 mm is used. $V^* = 14 \text{ cm}^3/\text{mol}$; $E^* = 510 \text{ kJ/mol}$.

Grain-size sensitive (GSS) and non-grain-size sensitive (NGSS) refer to the different temperature-velocity anelastic scaling models. The velocity melt scaling is $d\ln V_s/dF$, where F is percent melt porosity.

*Kreutzmann et al. (2004).

[†]Hammond and Humphreys (2000).

¹GSA Data Repository item 2008151, Appendix and Figures DR1–DR4, is available online at www.geosociety.org/pubs/ft2008.htm, or on request from editing@geosociety.org or Documents Secretary, GSA, P.O. Box 9140, Boulder, CO 80301, USA.

would violate the basalt petrology (Leeman et al., 2006) and isostatic constraints (Schutt and Humphreys, 2004). Based on these constraints, a 2–8 mm grain-size range is used for the plume layer.

For the NGSS anelasticity model, grain size is not an independent parameter. However, grain size mildly affects our velocity models via its effect on the matrix permeability, which is roughly proportional to the melt porosity. The calibrated material constants (V^* , E^* , preexponential constant, and frequency dependence exponent) are set to the values of Goes et al. (2000). The third anelastic model considered is based upon an empirical fit to tomographic oceanic shear wave velocity models, assumed thermal models, and continental xenoliths (Priestley and McKenzie, 2006). However, for a 1320 °C potential temperature mantle, an excess temperature of 100 °C at 100 km depth predicts an unrealistically low velocity of 3.2 km/s.

RESULTS

The results of our plume layer grid search fit to the Yellowstone hotspot track phase velocity data are summarized in Figures 2D and 2E and Table 1. To assess the statistical significance of the grid search results, the reduced χ^2_v misfit between the predicted and observed phase velocities is used. This statistic assumes 14 degrees of freedom based upon 17 phase velocity data and 3 model parameter constraints (calculated as the trace of the resolution matrix; Weeraratne et al., 2003). The χ^2_v from the grid search is primarily sensitive to the 25–80 s phase velocity data, which have small error bars (Fig. 3C). The poorer fit to the short period (<25 s) data is expected due to upper crustal velocity heterogeneity found along the Yellowstone hotspot track.

At a 68% confidence level, the GSS and NGSS anelastic models constrain the minimum excess temperature (i.e., for smallest 2 mm grain size) to be 150 °C and 120 °C. For the GSS models, the fit to the phase velocity data improves with increasing temperature and/or smaller grain size (Fig. 3D). At 95% confidence level, the GSS model using the Kreuzmann et al. (2004) melt-scaling requires excess temperatures of 70–200 °C for grain sizes of 2–8 mm. For the Humphreys and Hammond (2000) melt scaling, an excess temperature of 55–185 °C is required for grain sizes of 2–8 mm. The NGSS anelastic model χ^2_v values are larger (Fig. 2E) because this model does not produce low enough velocities to fit the observations, and a 95% confidence estimate does not exist for the large melt-velocity scaling relation of Hammond and Humphreys (2000).

A potential discriminant between the GSS and NGSS models is that for a given temperature, the GSS model predicts a lower shear wave quality factor (Q_s) with respect to the NGSS model (Figs. 3D, 3E). The lowest misfit GSS and NGSS models predict Q_s values of 15 and 25, respectively. However, without any estimates of the Q_s of the plume layer, we consider the Q_s predictions from both anelastic models as equally plausible.

Potential sources of error in our temperature estimates are a thicker lithospheric layer or a thicker plume layer. However, a thicker mantle lithosphere (currently 9 km) only requires greater plume temperatures, and we find that the χ^2_v values are insensitive to a thicker plume layer (see the Data Repository). Hence, the Yellowstone hotspot track phase velocity data truly require a profound low-velocity channel between 50 and 120 km depth.

DISCUSSION

Our melt porosity estimate of <0.2%–0.4% is reasonable (McKenzie, 1984) and consistent with the geochemical constraints provided by the late-stage basalts along the eastern Snake River Plain (Leeman et al., 2006). Our excess temperature estimate combined with the imaged width and assumed thickness of the plume layer permits a buoyancy flux estimate. Given that the plume is not spreading significantly beneath the lithosphere

(Schutt et al., 2008; Schutt and Humphreys, 2004; Waite et al., 2005), we assume that the upwelling rate of the plume is equal to the 2.1 cm/yr absolute North American plate motion. This vertical velocity rate in essence assumes that the plume material is being emplaced at the same rate that it is being advected horizontally by plate shear. These values define a buoyancy flux estimate of 0.03–0.1 Mg/s for a plume excess temperature of 70–200 °C, consistent with estimates from other methods (Waite, 2004). This buoyancy flux is much smaller than the 8 Mg/s buoyancy flux estimated for the Hawaiian plume (Sleep, 1990), but close to the 0.5–1.0 Mg/s flux proposed for the Eifel plume (Wüllner et al., 2006).

The excess temperature found by our analysis, combined with the tomographic and mantle velocity discontinuity results (Fee and Dueker, 2004; Waite et al., 2006; Yuan and Dueker, 2005), strongly suggests that the ultimate cause of the Yellowstone hotspot track is a thermal mantle plume. The absence of an observed lower mantle extension of the plume (Montelli et al., 2004a) suggests that the plume tail has either detached from the core-mantle boundary or has nucleated from an intermittent thermal boundary layer that may form about the 660 km discontinuity (Yuen et al., 1998). The low buoyancy flux may point to a mid-mantle plume (Goes et al., 2004). On the other hand, it has been shown that a subducting slab can nucleate a plume at the core-mantle boundary (Tan et al., 2002), and it is possible the Farallon slab may have played a role in the genesis of the Yellowstone plume. The relation of the Yellowstone plume to other contemporaneous magmatism in the Pacific Northwest remains to be elucidated: e.g., the High Lava Plains and the Columbia River Basalts may manifest plume material that has flowed along lithospheric thickness gradients (Jordan et al., 2004) and/or has also been advected by counterflow associated with the subducting Juan de Fuca plate (Humphreys et al., 2000).

To summarize, the very low velocity mantle plume layer beneath the Yellowstone hotspot track requires significant excess temperature with respect to an adiabatic mantle. Modeling shows that melt porosity cannot explain the velocity reduction. The minimum excess temperature of the plume material varies for the different anelastic and melt-velocity scaling models. The best-fitting GSS model for a 2 mm grain size requires >70 °C at 95% confidence. At 68% confidence, the two anelastic and two melt-velocity scaling models require an excess temperature >120 °C (Table 1). These excess temperature estimates are lower bounds, because our shear velocity model is an average of the plume's track over the past 8 m.y., and both heat diffusion and latent heat effects have removed heat from the plume layer.

ACKNOWLEDGMENTS

We thank Andrew Barth and three reviewers, Saskia Goes and two anonymous persons, for their helpful comments. We also thank Uli Faul for sharing a preprint of his work with us, and for helpful discussions. Schutt thanks the National Science Foundation (NSF) for support in the form of time to work on the project and for publication costs, as well as for NSF grant EAR-0409538.

REFERENCES CITED

- Armiénti, P., and Tarquini, S., 2002, Power law olivine crystal size distributions in lithospheric mantle xenoliths: *Lithos*, v. 65, p. 273–285, doi: 10.1016/S0024-4937(02)00195-0.
- Blackwell, D.D., Stelle, J.L., and Carter, L.S., 1991, Heat flow patterns of the North American continent: A discussion of the DNAG geothermal map of North America: *Neotectonics of North America: Geological Society of America: Geology of North America Decade Map*, v. 1, p. 498.
- Cammarano, F., Goes, S., Vacher, P., and Giardini, D., 2003, Inferring upper-mantle temperatures from seismic velocities: *Physics of the Earth and Planetary Interiors*, v. 138, p. 197–222, doi: 10.1016/S0031-9201(03)00156-0.
- Christiansen, R.L., Foulger, G.R., and Evans, J.R., 2002, Upper-mantle origin of the Yellowstone hotspot: *Geological Society of America Bulletin*, v. 114, p. 1245–1256, doi: 10.1130/0016-7606(2002)114.
- Dziewonski, A.M., and Anderson, D.L., 1981, Preliminary reference Earth model: *Physics of the Earth and Planetary Interiors*, v. 25, p. 297–356.

- Faul, U.H., and Jackson, H.R., 2005, The seismological signature of temperature and grain size variations in the upper mantle: *Earth and Planetary Science Letters*, v. 234, p. 119–134, doi: 10.1016/j.epsl.2005.02.008.
- Fee, D., and Dueker, K., 2004, Mantle transition zone topography and structure beneath the Yellowstone hotspot: *Geophysical Research Letters*, v. 31, doi: 10.1029/2004GL020636.
- Forsyth, D.W., and Li, A., 2005, Array-analysis of two-dimensional variations in surface wave phase velocity and azimuthal anisotropy in the presence of multipathing interference, in Levander, A., and Nolet, G., eds., *Seismic data analysis and imagine with global and local arrays: American Geophysical Union Geophysical Monograph 157*, p. 81–98.
- Goes, S., Govers, R., and Vacher, P., 2000, Shallow mantle temperatures under Europe from P and S wave tomography: *Journal of Geophysical Research*, v. 105, p. 11,153–11,169.
- Goes, S., Cammarano, F., and Hansen, U., 2004, Synthetic seismic signature of thermal mantle plumes: *Earth and Planetary Science Letters*, v. 218, p. 403–419.
- Grand, S.P., and Helmberger, D.V., 1984, Upper mantle shear structure of North America: *Royal Astronomical Society Geophysical Journal*, v. 76, p. 399–438.
- Hall, C.E., and Parmentier, E.M., 2003, Influence of grain size evolution on convective instability: *Geochemistry, Geophysics, Geosystems*, v. 4, doi: 10.1029/2002GC000308.
- Hammond, W.C., and Humphreys, E.D., 2000, Upper mantle seismic wave velocity: Effects of realistic partial melt geometries: *Journal of Geophysical Research*, v. 105, p. 10,975–10,986, doi: 10.1029/2000JB900041.
- Hirschmann, M.M., 2000, Mantle solidus: Experimental constraints and the effects of peridotite composition: *Geochemistry, Geophysics, Geosystems*, v. 1, 2000GC000070.
- Humphreys, E.D., Dueker, K.G., Schutt, D.L., and Smith, R.B., 2000, Beneath Yellowstone: evaluating plume and nonplume models using teleseismic images of the upper mantle: *GSA Today*, v. 10, p. 1–7.
- Jordan, B.T., Grunder, A.L., Duncan, R.A., and Deino, A.L., 2004, Geochronology of age-progressive volcanism of the Oregon High Lava Plains: Implications for the plume interpretation of Yellowstone: *Journal of Geophysical Research*, v. 109, B10202, doi: 10.1029/2003JB002776.
- Karato, S., 1993, Importance of anelasticity in the interpretation of seismic tomography: *Geophysical Research Letters*, v. 20, p. 1623–1626, doi: 10.1029/93GL01767.
- King, S.D., and Ritsema, J., 2000, African hot spot volcanism; small-scale convection in the upper mantle beneath cratons: *Science*, v. 290, p. 1137–1140.
- Kreutzmann, H., Schmeling, H., Jung, H., Ruedas, T., Marquart, G., and Bjarnason, I.T., 2004, Temperature and melting of a ridge-centered plume with application to Iceland. Part II: Predictions for electromagnetic and seismic observables: *Geophysical Journal International*, v. 159, p. 1097–1111, doi: 10.1111/j.1365–246X.2004.02397.x.
- Leeman, W.P., Schutt, D.L., and Hughes, S.S., 2006, Assessment of mantle thermal structure beneath the Snake River Plain–Yellowstone Hotspot: *Eos (Transactions, American Geophysical Union)*, v. 87, Fall meeting supplement, abs. V33D-06.
- Lowry, A.R., Ribe, N.M., and Smith, R.B., 2000, Dynamic elevation of the Cordillera, western United States: *Journal of Geophysical Research*, v. 105, p. 23,371–23,390, doi: 10.1029/2000JB900182.
- Lum, C.C.L., Fitton, J.G., Leeman, W.P., Foland, K.A., and Kargel, J.A., 1989, Isotopic variations in continental basaltic lavas as indicators of mantle heterogeneity: Examples from the western US Cordillera: *Journal of Geophysical Research*, v. 94, p. 7871–7884, doi: 10.1029/JB094iB06p07871.
- McKenzie, D.M., 1984, The generation and compaction of partially molten rock: *Journal of Petrology*, v. 25, p. 713–765.
- McQuarrie, N., and Rodgers, D.W., 1998, Subsidence of a volcanic basin by flexure and lower crustal flow: The eastern Snake River Plain, Idaho: *Tectonics*, v. 17, p. 203–220, doi: 10.1029/97TC03762.
- Minster, J.B., and Anderson, D.L., 1981, A model of dislocation-controlled rheology for the mantle: *Royal Society of London Philosophical Transactions, ser. A*, v. 299, p. 319–356, doi: 10.1098/rsta.1981.0025.
- Montelli, R., Nolet, G., Dahlen, F.A., Masters, G., Engdahl, E.R., and Hung, S.H., 2004a, Finite-frequency tomography reveals a variety of plumes in the mantle: *Science*, v. 303, p. 338–343, doi: 10.1126/science.1092485.
- Montelli, R., Nolet, G., Masters, G., Dahlen, F.A., and Hung, S.H., 2004b, Global P and PP traveltimes tomography: rays versus waves: *Geophysical Journal International*, v. 158, p. 637–654, doi: 10.1111/j.1365–246X.2004.02346.x.
- Nishimura, T., and Forsyth, D.W., 1989, The anisotropic structure of the upper mantle in the Pacific: *Geophysical Journal*, v. 96, p. 203–229.
- Priestley, K., and McKenzie, D., 2006, The thermal structure of the lithosphere from shear wave velocities: *Earth and Planetary Science Letters*, v. 244, p. 285–301, doi: 10.1016/j.epsl.2006.01.008.
- Priestley, K.F., and Tilman, F.J., 1999, Shear-wave of the lithosphere above the Hawaiian hotspot from two-station Rayleigh wave phase velocity measurements: *Geophysical Research Letters*, v. 26, p. 1493–1496, doi: 10.1029/1999GL900299.
- Putirka, K.D., 2005, Mantle potential temperatures at Hawaii, Iceland, and the mid-ocean ridge system, as inferred from olivine phenocrysts; evidence for thermally driven mantle plumes: *Geochemistry, Geophysics, Geosystems*, v. 6, p. 14.
- Schutt, D.L., and Humphreys, E.D., 2003, P and S wave velocity and Vp/Vs in the wake of the Yellowstone hotspot: *Journal of Geophysical Research*, v. 108, B01305, doi: 10.1029/2003JB002442.
- Schutt, D.L., and Lesher, C.E., 2006, The effects of melt depletion on the density and seismic velocity of garnet and spinel lherzolite: *Journal of Geophysical Research*, v. 111, B05401, doi: 10.1029/2003JB002950.
- Schutt, D.L.K.D., and Yuan, H., 2008, Crustal and upper mantle velocity structure of the Yellowstone hot spot and surroundings: *Journal of Geophysical Research*, v. 113, B03310, doi: 10.1029/2007JB005109.
- Sleep, N.H., 1990, Hotspots and mantle plumes: Some phenomenology: *Journal of Geophysical Research*, v. 95, p. 6715–6736, doi: 10.1029/JB095iB05p06715.
- Tan, E., Gurnis, M., and Han, L., 2002, Slabs in the lower mantle and their modulation of plume formation: *Geochemistry, Geophysics, Geosystems*, v. 3, 1067, doi: 10.1029/2001GC000238.
- Turcotte, D., and Schubert, G., 2002, *Geodynamics*: Cambridge, Cambridge University Press, 456 p.
- Waite, G., Schutt, D.L., and Smith, R.B., 2005, Shear wave anisotropy of the Yellowstone hotspot: *Journal of Geophysical Research*, v. 110, B11304, doi: 10.1029/2004JB003501.
- Waite, G., Smith, R.B., and Allen, R.M., 2006, Vp and Vs structure of the Yellowstone Hotspot upper mantle from teleseismic tomography: Evidence for an upper mantle plume: *Journal of Geophysical Research*, v. 111, B04303, doi: 10.1029/2005JB003867.
- Weeraratne, D.S., Forsyth, D.W., Fischer, K.M., and Nyblade, A.A., 2003, Evidence for an upper mantle plume beneath the Tanzanian craton from Rayleigh wave tomography: *Journal of Geophysical Research*, v. 108, no. B9, 2427, doi: 10.1029/2002JB002273.
- Weeraratne, D.S., Forsyth, D.W., Yang, Y., and Webb, S.C., 2007, Rayleigh wave tomography beneath intraplate volcanic ridges in the South Pacific: *Journal of Geophysical Research*, v. 112, B06303, doi: 10.1029/2006JB004403.
- Wilshire, H.G., Meyer, C.E., Nakata, J.K., Calk, L.C., Shervais, J.W., Nielson, J.E., and Schwarzman, E.C., 1988, Mafic and ultramafic xenoliths from volcanic rocks of the western United States: U.S. Geological Survey Professional Paper 1443, 179 p.
- Wüllner, U., Christensen, U.R., and Jordan, M., 2006, Joint geodynamical and seismic modelling of the Eifel plume: *Geophysical Journal International*, v. 165, p. 357–372.
- Yuan, H., and Dueker, K., 2005, Teleseismic P-wave tomogram of the Yellowstone plume: *Geophysical Research Letters*, v. 32, L07304, doi: 10.1029/2004GL022056. Yuan.
- Yuen, D.A., Cserepes, L., and Schroeder, B.A., 1998, Mesoscale structures in the transition zone: Dynamical consequences of boundary layer activities: *Earth: Planets and Space*, v. 50, p. 1035–1045.

Manuscript received 25 January 2008

Revised manuscript received 26 April 2008

Manuscript accepted 1 May 2008

Printed in USA